ARTICLES

Journal of Semiconductors
(2022) 43, 112302
doi: 10.1088/1674-4926/43/11/112302

JOS

Ag-catalyzed GaSb nanowires for flexible near-infrared photodetectors

Zixu Sa[1], Fengjing Liu[1], Dong Liu[1], Mingxu Wang[1], Jie Zhang[1], Yanxue Yin[1], Zhiyong Pang[1, †], Xinming Zhuang[1], Peng Wang[2, †], and Zaixing Yang[1, †]

[1]School of Physics, School of Microelectronics, State Key Laboratory of Crystal Materials, Shandong University, Jinan 250100, China

[2]College of Electronic and Information Engineering, Shandong University of Science and Technology, Qingdao 266590, China

Abstract: High-quality narrow bandgap semiconductors nanowires (NWs) challenge the flexible near-infrared (NIR) photodetectors in next-generation imaging, data communication, environmental monitoring, and bioimaging applications. In this work, complementary metal oxide semiconductor-compatible metal of Ag is deposited on glass as the growth catalyst for the surfactant-assisted chemical vapor deposition of GaSb NWs. The uniform morphology, balance stoichiometry, high-quality crystallinity, and phase purity of as-prepared NWs are checked by scanning electron microscopy, energy dispersive X-ray spectroscopy, high-resolution transmission electron microscopy, and X-ray diffraction. The electrical properties of as-prepared NWs are studied by constructing back-gated field-effect-transistors, displaying a high I_{on}/I_{off} ratio of 10^4 and high peak hole mobility of 400 $cm^2/(V{\cdot}s)$. Benefiting from the excellent electrical and mechanical flexibility properties, the as-fabricated NW flexible NIR photodetector exhibits high sensitivity and excellent photoresponse, with responsivity as high as 618 A/W and detectivity as high as 6.7×10^{10} Jones. Furthermore, there is no obvious decline in NIR photodetection behavior, even after parallel and perpendicular folding with 1200 cycles.

Key words: near-infrared photodetector; flexible; GaSb nanowires; CMOS-compatible catalyst

Citation: Z X Sa, F J Liu, D Liu, M X Wang, J Zhang, Y X Yin, Z Y Pang, X M Zhuang, P Wang, and Z X Yang, Ag-catalyzed GaSb nanowires for flexible near-infrared photodetectors[J]. *J. Semicond.*, 2022, 43(11), 112302. https://doi.org/10.1088/1674-4926/43/11/112302

1. Introduction

In the past few decades, flexible near-infrared (NIR) photodetectors have attracted significant attention in imaging, data communication, environmental monitoring, and bioimaging applications[1–4]. However, scalability, sensitivity and mechanical stability challenge the selection of channel semiconductors and device fabrication of flexible NIR photodetectors[5]. Due to the excellent mechanical flexibility in comparison to the typical thin film or bulk counterparts, low-dimensional organic and inorganic semiconductors, such as one-dimensional (1D) nanowires (NWs) and two-dimensional nanosheets, have recently been attempted to realize flexible NIR photodetectors[6–11]. Apart from the excellent mechanical flexibility, 1D NWs also have great advantages in large surface-to-volume ratio, high carrier mobility, and good light absorption ability, displaying competitive application in high-sensitive, high-durable and versatile flexible NIR photodetectors[12–17]. For example, flexible $CH_3NH_3PbI_3$ NW NIR photodetector has been fabricated by Tao *et al.*, displaying a responsivity of 0.227 A/W at the low light intensity of 1×10^8 W/cm^2 and maintaining a good photoresponse up to 1500 folding cycles[10]. In the case of inorganic NWs, Bi_2O_2Se NWs have been adopted to fabricate flexible NIR photodetector by Li *et al.*, demonstrating a remarkable photoresponse and stable characteristics with 1200 bending cycles[8].

Narrow bandgap semiconductors NWs of III–Sb have been considered as promising candidates for next-generation electronic and photoelectronic nanodevices. With the narrow direct bandgap of 0.726 eV and high hole mobility of 1000 $cm^2/(V{\cdot}s)$, GaSb NW is certainly an active channel semiconductor for flexible NIR photodetectors. Up to now, vapor growth methods of molecular beam epitaxy, metal-oxide vapor phase epitaxy, metal-oxide chemical vapor deposition, and chemical vapor deposition (CVD), and so on have been universally developed for the growth of GaSb NWs, followed by the famous vapor–solid–solid or vapor–liquid–solid (VLS) growth mechanism[18–21]. It is worth pointing out that a surfactant-assisted CVD method recently has been developed to prevent the sidewall growth of GaSb NWs, resulting in the successful control of diameter, length, growth orientation, crystallinity, hole concentration and so on[22–26]. During the developed surfactant-assisted CVD process, complementary metal oxide semiconductor (CMOS)-incompatible and -compatible metals of Au, Sn, Pd and Cu have been deposited on substrates to serve as the growth catalysts[22, 25–27].

Although the NIR photodetection behavior of GaSb NWs has been studied, there is still very limited work on their flexible photodetectors[25, 27, 28]. In this work, CMOS-compatible metal of Ag is first adopted as the growth catalyst for GaSb NWs during a surfactant-assisted CVD process. The as-prepared GaSb NWs show high density, smooth surface, balance stoichiometry, uniform diameter and good crystalline. When configuring into the famous back-gated field-effect-transist-

Correspondence to: Z Y Pang, pang@sdu.edu.cn; P Wang, phywangp@sdust.edu.cn; Z X Yang, zaixyang@sdu.edu.cn
Received 13 MAY 2022; Revised 9 JUNE 2022.
©2022 Chinese Institute of Electronics

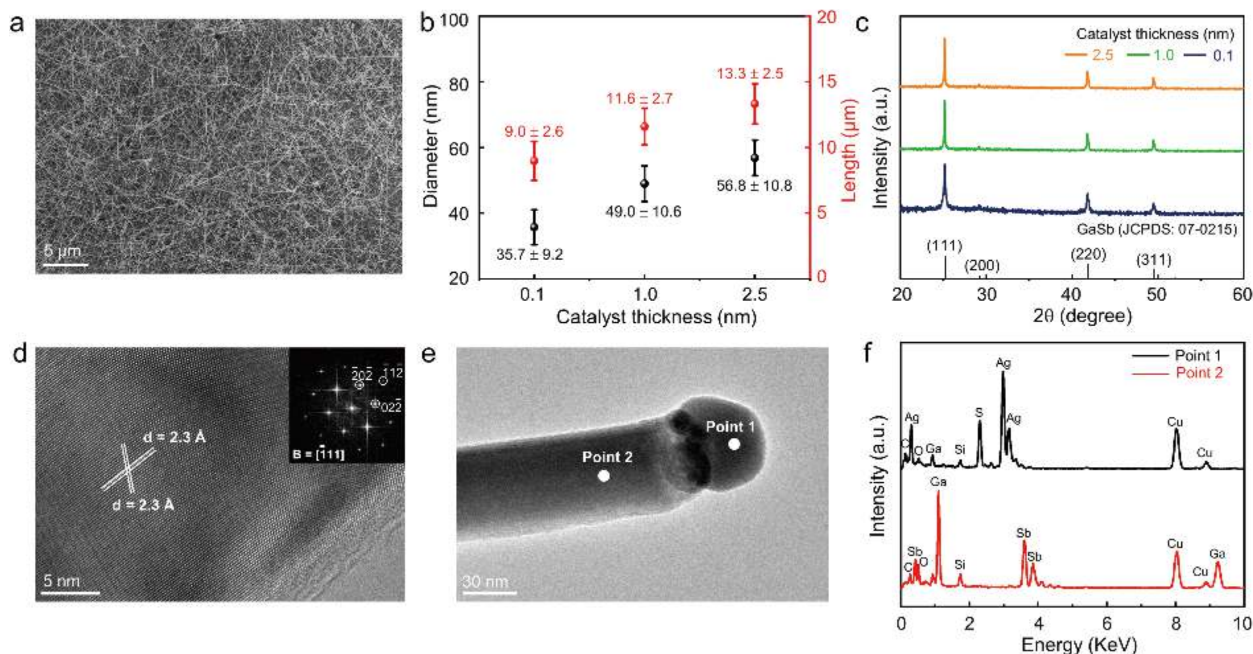

Fig. 1. (Color online) Controllable growth of GaSb NWs by using the CMOS-compatible metal of Ag as the growth catalyst. (a–c) SEM image, diameter and length statistics, and XRD patterns of as-prepared Ag-catalyzed GaSb NWs. (d) HRTEM image of GaSb NW, insert is FFT image. (e) Scanning TEM image of an individual GaSb NW. (f) EDS of NW tip and body.

ors (FETs), GaSb NWs exhibit excellent electrical performance with a high I_{on}/I_{off} ratio (10^4) and high peak hole mobility (400 cm²/(V·s)). Additionally, the as-prepared NWs exhibit good NIR photodetection performance, such as high responsivity of 881 A/W, detectivity of 8.5×10^{10} Jones and fast response speed under 1550 nm illumination. Furthermore, the as-fabricated flexible photodetectors also hold the excellent photoresponse to NIR. After the parallel and perpendicular folding with 1200 cycles, the characteristics of flexible photodetectors exhibit no obvious decline, strongly revealing the promising advantage in robust mechanical flexibility, electrical and photoelectrical stability and bending endurance.

2. Results and discussion

In this work, CMOS-compatible metal of Ag is deposited on amorphous glass as the growth catalyst during the developed surfactant-assisted CVD process. The detailed growth process can be found in supplementary material. From the scanning electron microscopy (SEM) image in Fig. 1(a) and Fig. S1, all the as-prepared samples are uniform NWs with high density and smooth surfaces. As shown in Fig. 1(b), as the thickness of Ag catalyst films increases from 0.1, 1.0, to 2.5 nm, the diameter of as-prepared NWs increases from 35.7 ± 9.2, 49.0 ± 10.6, to 56.8 ± 10.8 nm, while the corresponding length increases from 9.0 ± 2.6, 11.6 ± 2.7 to 13.3 ± 2.5 μm. All of the diameters and lengths are estimated from the corresponding SEM images, as shown in Fig. S1. As verified by X-ray diffraction (XRD) in Fig. 1(c), the as-prepared NWs are the pure zinc blende crystal structure (JCPDS Card No. 07–0215) of GaSb. Furthermore, high-resolution transmission electron microscope (HRTEM) is adopted to characterize the microstructure of Ag-catalyzed GaSb NWs. The clear lattice spacings of 2.2 Å are assigned to $(02\bar{2})$ and $(\bar{2}0\bar{2})$ planes, indicating the good crystallinity of as-prepared GaSb NW grows along ⟨211⟩ direction. This result is further confirmed by the corresponding reciprocal lattice space extracted by fast Fourier transform (FFT). At the same time, a spherical catalytic seed is observed on the tip of NW (as shown in Fig. 1(e)), inferring a VLS growth mechanism[22, 26]. The composition of catalytic seed and NW body are then checked by energy dispersive X-ray spectroscopy (EDS) in Fig. 1(f). The spherical catalytic seed contains Ag, Ga and S elements, whereas the NW body shows a balanced stoichiometry of Ga : Sb ~ 1 : 1. In other words, high-quality GaSb NWs with controlled diameters and lengths are prepared successfully by using CMOS-compatible metal of Ag as the growth catalyst during a surfactant-assisted CVD process.

After the successful growth of high-quality GaSb NWs, back-gated FETs are constructed to investigate the corresponding electrical properties, as shown in Fig. 2. The linear output characteristic of Fig. 2(a) confirms the ohmic-like contact of as-constructed GaSb NWFET with Ni electrodes. As depicted in Fig. 2(b) and Fig. S2, the typical transfer curve exhibits the p-type conduction behavior of as-prepared Ag-catalyzed GaSb NW with a high I_{on}/I_{off} ratio of 10^4, which is similar to the previous reports[21, 25]. The hysteresis observed in the transfer curve may be caused by the surface states or dielectric interfaces, which could be weakened further by surface decoration or passivation, construction of core-shell structure and introduction of stress, and so on[29–33]. The field-effect mobility of as-constructed back-gated NWFET is then calculated by the square law model. The field-effect mobility μ can be calculated from $\mu = g_m \times (L^2/C_{OX}) \times (1/V_{DS})$, where g_m is the low-bias (i.e., V_{DS} = 0.1 V) transconductance extracted from the transfer characteristics $g_m = (dI_{DS})/(dV_{GS})|V_{DS}$, in which L is the channel length, and C_{OX} is the gate capacitance obtained from the finite element analysis software COMSOL for different NW diameters[25, 29, 34, 35]. In this case, as shown in Fig. 2(c), the corresponding peak hole mobility reaches up to 400 cm²/(V·s), with NW diameter of 30 nm and channel length of 5 μm, approaching to the theoretical mobility limitation with a hole concentration of 10^{18} cm^{-3}[36]. In addition, it is worth pointing out that

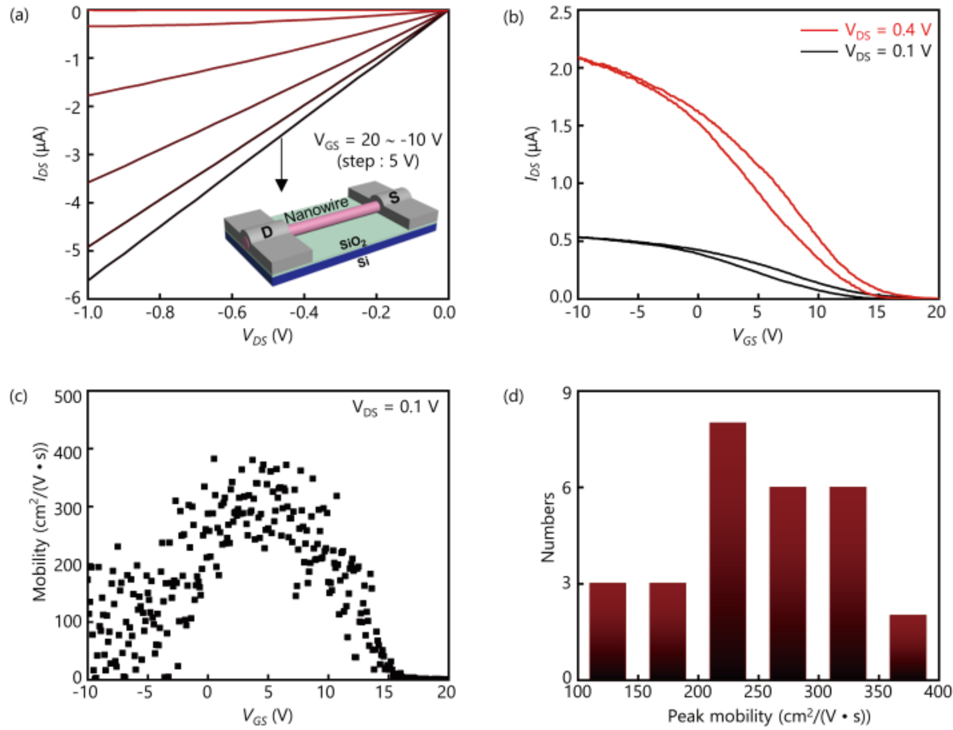

Fig. 2. (Color online) Electrical properties of the as-prepared Ag-catalyzed GaSb NWs. (a, b) Output and transfer characteristics of as-constructed GaSb NWFET. The inset is the corresponding device schematics. (c) Hole mobility of the corresponding NWFET. (d) Peak hole mobility statistic of as-constructed NWFETs.

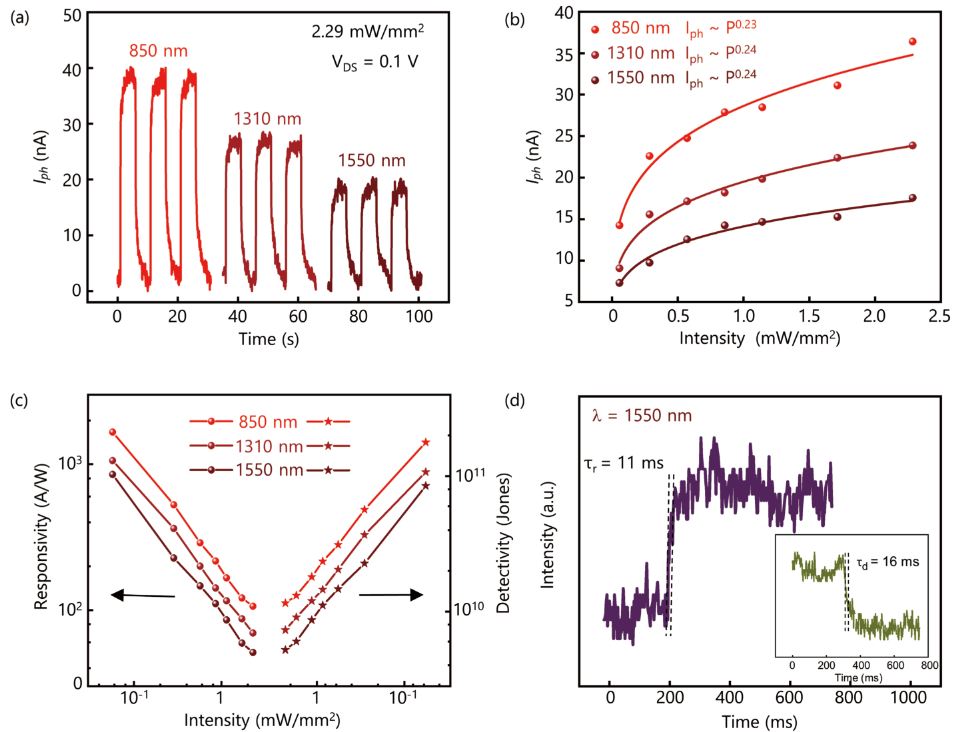

Fig. 3. (Color online) NIR photodetection behaviors of as-prepared Ag-catalyzed GaSb NWs. (a) I–t curves of GaSb photodetector under different illuminations of λ = 850 nm to λ = 1550 nm at 0.1 V. (b, c) Incident light intensity-dependent photocurrent, responsivity and detectivity, respectively. (d) Rise and decay time of the as-fabricated photodetector under 1550 nm laser illumination.

a wire-to-wire variation is observed in peak hole mobility statistic of Fig. 2(d), contributing from the dependence of electrical properties on NW diameters, orientations, surface roughness and others. Nevertheless, the as-prepared Ag-catalyzed GaSb NWs exhibit impressive electrical performance, promising the next-generation electronic devices.

Benefiting from the narrow bandgap, the NIR photodetection behaviors of as-prepared Ag-catalyzed GaSb NWs are then systematically investigated by constructing the famous metal-semiconductor-metal devices on a hard substrate. The I–t curves of GaSb NW photodetectors under different illuminations of λ = 850 nm to λ = 1550 nm are presented in Fig. 3(a)

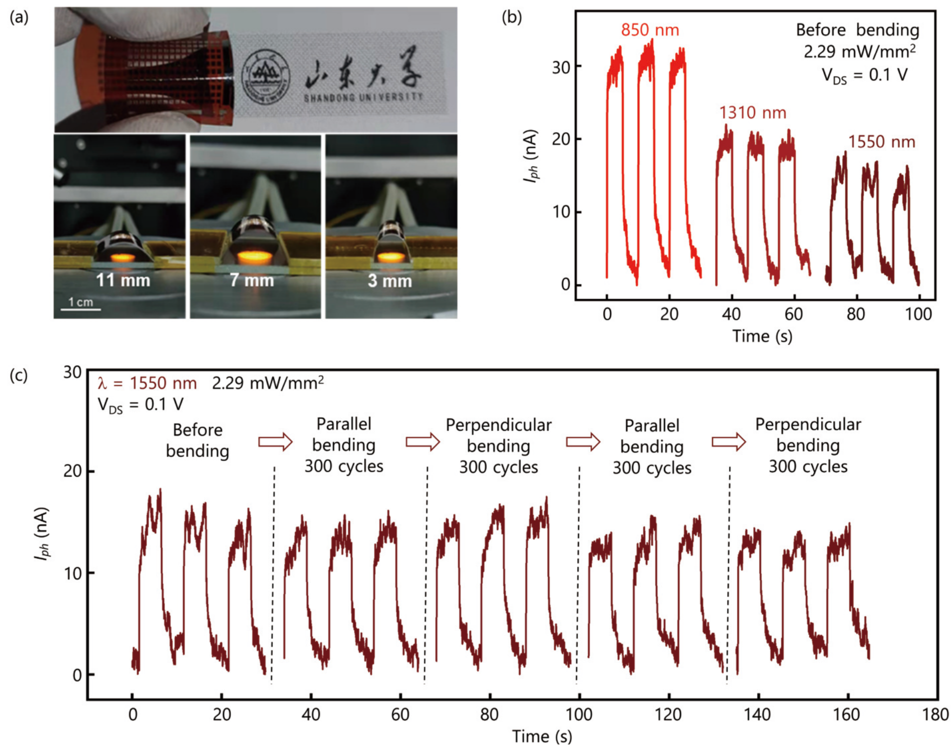

Fig. 4. (Color online) NIR photodetection behaviors of as-fabricated GaSb NW flexible photodetector. (a) The photographs of as-fabricated flexible photodetector under different bending radius. (b) The time-resolved photoresponse of flexible photodetector under the illuminations of 850, 1310, and 1550 nm lasers with 0.1 V bias before bending. (c) The time-resolved photoresponse of photodetector under the illumination of 1550 nm laser after bending different cycles.

and Figs. S3(a)–S3(c). Although fluctuation is observed, it is clear that the photocurrent (defined as $I_{ph} = |I_{light}| - |I_{dark}|$) is effectively modulated by periodic monochromatic laser illumination, which reveals that the as-fabricated photodetector shows excellent photoresponse to NIR bands and reproducible dynamic stability. Fig. 3(b) depicts the dependent relationship of the photocurrent on the incident light power intensity which obeys the power law $I_{ph} \sim P^{\beta}$, where I_{ph} is the photocurrent, P is the light intensity and β is the empirical value[37–39]. Therefore, β = 0.23, 0.24, and 0.24 are fitted by the relationships according to the data of 850, 1310, and 1550 nm, respectively. Because the wavelength of incident lights is much larger than the diameter of NWs, the absorption difference of NWs under the illuminations of three incident lights is neglectable, resulting in the similar values of β. It is worth pointing out that the value of β reflects the complex process of electron-hole generation, trapping, and recombination within the NW[39, 40]. Meanwhile, the GaSb NW photodetectors also display good static detection performance, as shown in Fig. S3(d). Therefore, further efforts can be focused on the current fluctuation suppressing by surface passivation or the construction of core-shell NWs[30, 41, 42].

Notably, responsivity (R) and detectivity (D^*) are two essential parameters for a photodetector, R indicates the response efficiency of the photodetector to the optical signal and D^* characterizes the minimum light signal that the photodetector can detect[31, 42]. R can be defined as $R = I_{ph}/(PA)$, in which I_{ph} is the photocurrent, P is the incident power density, and A is the effective irradiated area of the corresponding photodetector. D^* can be defined as $D^* = RA^{1/2}/(2eI_{dark})^{1/2}$, where e is the electronic charge and I_{dark} is dark current[38]. In this case, as shown in Fig. 3(c), the R reaches up to 881 A/W and the D^* reaches up to 8.5 × 10^{10} Jones under the illumination of 1550 nm laser with an intensity of 0.57 mW/mm^2, while R and D^* reach 1059 A/W, 1.1 × 10^{11} Jones and 1661 A/W, 1.8 × 10^{11} Jones for the NIRs of 1310 and 850 nm, respectively. Furthermore, another essential parameter for photodetector is the response time, which can be defined as the rising time (τ_r) and decay time (τ_d) for the photocurrent to increase/decrease from 10/90% to 90/10%, respectively[25, 42]. From the temporal photoresponse curve of GaSb NW photodetector under the illumination of 1550 nm laser in Fig. 3(d), the τ_r can be calculated as 11 ms and the τ_d can be calculated as 16 ms. In short, the as-fabricated Ag-catalyzed GaSb NW NIR photodetector exhibits excellent photoresponse performance on a hard substrate, promising the next-generation photoelectric devices.

With the excellent photodetection performance, it is necessary to make use of as-prepared Ag-catalyzed GaSb NWs to fabricate flexible NIR photodetectors. In general, the surface roughness of flexible substrates is challenging the fabrication of high-performance NIR photodetectors[2, 6]. After the optimization of photolithography process, GaSb NW flexible photodetectors on polyimide (PI) substrates are successfully fabricated, as shown in Fig. 4(a). The as-fabricated GaSb NW flexible photodetectors exhibit good bendability and flexibility, and even maintain good shape at bending radius of 3 mm as shown in Fig. 4(a). As presented in Fig. 4(b), the GaSb NW flexible photodetector shows good and stable photoresponse to NIR lasers of different wavelengths before bending. The R is as high as 618 A/W and D^* is as high as 6.7 × 10^{10} Jones under the illumination of 1550 nm laser, as

Table 1. Photodetection performance comparison of GaSb NW photodetector.

GaSb NW	Devices substrate	Photodetection wavelength (nm)	V_{ds} (V)	R (A/W)	D (Jones)	Response time (ms)	Ref.
Single	Hard	1550	0.1	851	8.5×10^{10}	11/16	This work
	Flexible	1550	0.1	618	6.7×10^{10}	–	
Single	Hard	800	2	443	2.8×10^{9}	80/90	[27]
Single	Hard	808	5	722	5.9×10^{12}	8700	[28]
	Flexible	808	5	–	4.9×10^{12}	–	
Single	Hard	1550	1	77.3	1.2×10^{10}	–	[43]
Single	Hard	1310	1	1600	5.7×10^{9}	4.5/12	[21]
Single	Hard	1550	1	61	8.7×10^{7}	0.195/0.38	[25]
Single	Hard	1550	1	939	1.1×10^{11}	50/900	[44]

shown in Fig. S4(a), which is comparable to the performance of device on hard substrate. It is worthwhile to note that even under the small bias of 0.1 V, the as-fabricated GaSb NW photodetector still exhibits competitive NIR photodetection performances on both hard and flexible substrates, as shown in Table 1. The photodetection performance of flexible GaSb NWs photodetectors can be further optimized by using the smoother and softer flexible substrates[6, 28]. Apart from flexibility, the bending endurance is another indispensable factor restricting the development and practical application of the flexible devices[12, 45, 46]. To more realistically test the bending endurance, the flexible photodetector is bent in parallel and perpendicular orientation alternatively, as shown in Fig. 4(c). It is obviously that the photodetection performance of GaSb NW flexible photodetector shows no obvious decline after the multiple bending cycles. Even after bending with 1200 cycles, the GaSb NW flexible photodetector still maintains satisfactory detection performance for 850, 1310, and 1550 nm NIR lights as shown in Figs. S4(b) and S4(c). These results reveal that the as-fabricated flexible NIR photodetector enabled by Ag-catalyzed GaSb NW exhibits outstanding mechanical flexibility, photoelectronic stability and bending endurance, greatly promoting the development of NWs flexible photodetectors.

3. Conclusion

In summary, high-quality GaSb NWs have been prepared successfully by adopting the CMOS-compatible metal of Ag as the growth catalyst during a surfactant-assisted CVD process. The as-prepared NWs show high density, smooth surface, balance stoichiometry, uniform diameter and good crystallinity. They also exhibit the expected high peak hole mobility of 400 $cm^2/(V{\cdot}s)$, high responsivity of 881 A/W, high detectivity of 8.5×10^{10} Jones and fast response speed under the illumination of 1550 nm. When configured into the flexible photodetectors, GaSb NWs have excellent NIR photodetection behaviors, along with high mechanical flexibility and bending endurance. All of these results promote the use of as-studied high-quality GaSb NWs catalyzed by Ag for the next-generation high-performance flexible NIR photodetectors.

Acknowledgements

Z.X. Sa and F.J. Liu contributed equally to this work. We acknowledge the National Key R&D Program of China (No. 2017YFA0305500), National Natural Science Foundation of China (Nos. 61904096, 11504207), Taishan Scholars Program of Shandong Province (No. tsqn201812006), Shandong University Youth Innovation Supporting Program (No. 2019-KJN020), Shandong University Multidisciplinary Research and Innovation Team of Young Scholars (No. 2020QNQT015), and "Outstanding youth scholar and Qilu young scholar" programs of Shandong University.

Appendix A. Supplementary material

Supplementary materials to this article can be found online at https://doi.org/10.1088/1674-4926/43/11/112302.

References

[1] Ran W H, Wang L L, Zhao S F, et al. An integrated flexible all-nanowire infrared sensing system with record photosensitivity. Adv Mater, 2022, 32, 1908419

[2] Wei S L, Wang F, Zou X M, et al. Flexible quasi-2D perovskite/IGZO phototransistors for ultrasensitive and broadband photodetection. Adv Mater, 2020, 32, 1907527

[3] Li Z Y, Trendafilov S, Zhang F L, et al. Broadband GaAsSb nanowire array photodetectors for filter-free multispectral imaging. Nano Lett, 2021, 21, 7388

[4] Yip S, Shen L F, Ho J C. Recent advances in flexible photodetectors based on 1D nanostructures. J Semicond, 2019, 40, 111602

[5] Xie C, Yan F. Flexible photodetectors based on novel functional materials. Small 2017, 13, 1701, 822

[6] Lou Z, Shen G Z. Flexible photodetectors based on 1D inorganic nanostructures. Adv Sci, 2016, 3, 1500287

[7] Li P, Hao Q Y, Liu J D, et al. Flexible photodetectors based on all-solution-processed Cu electrodes and InSe nanoflakes with high stabilities. Adv Funct Mater, 2021, 32, 2108261

[8] Li J, Wang Z X, Chu J W, et al. Oriented layered Bi_2O_2Se nanowire arrays for ultrasensitive photodetectors. Appl Phys Lett, 2019, 114, 151104

[9] Wu D J, Zhou H, Song Z H, et al. Welding perovskite nanowires for stable, sensitive, flexible photodetectors. ACS Nano, 2020, 14, 2777

[10] Tao J Y, Xiao Z J, Wang J F, et al. A self-powered, flexible photodetector based on perovskite nanowires with Ni-Al electrodes. J Alloys Compd, 2020, 845, 155311

[11] Lou Z, Yang X L, Chen H R, et al. Flexible ultraviolet photodetectors based on ZnO–SnO_2 heterojunction nanowire arrays. J Semicond, 2018, 39, 024002

[12] Li D P, Yip S, Li F Z, et al. Flexible near-infrared InGaSb nanowire array detectors with ultrafast photoconductive response below 20 μs. Adv Opt Mater, 2020, 8, 2001201

[13] Rezaei M, Bianconi S, Lauhon L, et al. A new approach to designing high-sensitivity low-dimensional photodetectors. Nano Lett, 2021, 21, 9838

[14] Barrigon E, Heurlin M, Bi Z, et al. Synthesis and applications of III-V nanowires. Chem Rev, 2019, 119, 9170

[15] Yuan X M, Pan D, Zhou Y J, et al. Selective area epitaxy of III–V nanostructure arrays and networks: growth, applications, and fu-

ture directions. Appl Phys Rev, 2021, 8, 021302
[16] Zuo X R, Li Z Y, Wong W W, et al. Design of InAs nanosheet arrays with ultrawide polarization-independent high absorption for infrared photodetection. Appl Phys Lett, 2022, 120, 071109
[17] Zhong Z Q, Li X L, Wu J, et al. Wavelength-tunable InAsP quantum dots in InP nanowires. Appl Phys Lett, 2019, 115, 053101
[18] Ji X H, Yang X G, Yang T. Self-catalyzed growth of vertical GaSb nanowires on InAs stems by metal-organic chemical vapor deposition. Nanoscale Res Lett, 2017, 12, 428
[19] Wen L J, Pan D, Liao D X, et al. Foreign-catalyst-free GaSb nanowires directly grown on cleaved Si substrates by molecular-beam epitaxy. Nanotechnology, 2020, 31, 155601
[20] Jeppsson M, Dick K A, Nilsson H A, et al. Characterization of GaSb nanowires grown by MOVPE. J Cryst Growth, 2008, 310, 5119
[21] Yin Y X, Guo Y N, Liu D, et al. Substrate-free chemical vapor deposition of large-scale III-V nanowires for high-performance transistors and broad-spectrum photodetectors. Adv Opt Mater, 2022, 10, 2102291
[22] Yang Z X, Han N, Fang M, et al. Surfactant-assisted chemical vapour deposition of high-performance small-diameter GaSb nanowires. Nat Commun, 2014, 5, 5249
[23] Yang Z X, Yin Y X, Sun J M, et al. Chalcogen passivation: an in-situ method to manipulate the morphology and electrical property of GaAs nanowires. Sci Rep, 2018, 8, 6928
[24] Yang Z X, Liu L Z, Yip S, et al. Complementary metal oxide semiconductor-compatible, high-mobility, 111-oriented GaSb nanowires enabled by vapor-solid-solid chemical vapor deposition. ACS Nano, 2017, 11, 4237
[25] Sun J M, Peng M, Zhang Y S, et al. Ultrahigh hole mobility of Sn-catalyzed GaSb nanowires for high speed infrared photodetectors. Nano Lett, 2019, 19, 5920
[26] Han N, Wang Y, Yang Z X, et al. Controllable III-V nanowire growth via catalyst epitaxy. J Mater Chem C, 2017, 5, 4393
[27] Luo T, Liang B, Liu Z, et al. Single-GaSb-nanowire-based room temperature photodetectors with broad spectral response. Sci Bull, 2015, 60, 101
[28] Zhang K, Chai R Q, Shi R L, et al. Self-catalyzed growth of GaSb nanowires for high performance ultraviolet-visible-near infrared photodetectors. Sci China Mater, 2019, 63, 383
[29] Sun J M, Zhuang X M, Fan Y B, et al. Toward unusual-high hole mobility of p-channel field-effect-transistors. Small, 2021, 17, 2102323
[30] Liu D, Liu F J, Liu Y, et al. Schottky-contacted high-performance GaSb nanowires photodetectors enabled by lead-free all-inorganic perovskites decoration. Small, 2022, 18, 2200415
[31] Miao J S, Hu W D, Guo N, et al. Single InAs nanowire room-temperature near-infrared photodetectors. ACS Nano, 2014, 8, 3628
[32] Al-Zahrani S, Pal J, Migliorato M A, et al. Piezoelectric field enhancement in III-V core–shell nanowires. Nano Energy, 2015, 14, 382
[33] Holmer J, Zeng L, Kanne T, et al. Enhancing the nir photocurrent in single GaAs nanowires with radial p-i-n junctions by uniaxial strain. Nano Lett, 2021, 21, 9038
[34] Ford A C, Ho J C, Chueh Y L, et al. Diameter-dependent electron mobility of InAs nanowires. Nano Lett, 2009, 9, 360
[35] Burke R A, Weng X J, Kuo M W, et al. Growth and characterization of unintentionally doped GaSb nanowires. J Electron Mater, 2010, 39, 355
[36] Kranzer D. Mobility of holes of zinc-blende III-V and II-VI compounds. Phys Status Solidi A, 1974, 26, 11
[37] Jie J S, Zhang W J, Jiang Y, at al. Photoconductive characteristics of single-crystal CdS nanoribbons. Nano Lett, 2006, 6, 1887
[38] Fang H H, Hu W D, Wang P, et al. Visible light-assisted high-performance mid-infrared photodetectors based on single InAs nanowire. Nano Lett, 2016, 16, 6416
[39] Kind H, Yan H Q, Messer B, et al. Nanowire ultraviolet photodetectors and optical switches. Adv Mater, 2002, 14, 158
[40] Liu X, Gu L L, Zhang Q P, et al. All-printable band-edge modulated ZnO nanowire photodetectors with ultra-high detectivity. Nat Commun, 2014, 5, 4007
[41] Zheng D S, Wang J L, Hu W D, et al. When nanowires meet ultrahigh ferroelectric field-high-performance full-depleted nanowire photodetectors. Nano Lett, 2016, 16, 2548
[42] Liu L, Wu L M, Wang A W, et al. Ferroelectric-gated InSe photodetectors with high on/off ratios and photoresponsivity. Nano Lett, 2020, 20, 6666
[43] Ren Z H, Wang P, Zhang K, et al. Short-wave near-infrared polarization sensitive photodetector based on GaSb nanowire. IEEE Electron Device Lett, 2021, 42, 549
[44] Zhang K, Ren Z H, Cao H C, et al. Near-infrared polarimetric image sensors based on ordered sulfur-passivation GaSb nanowire arrays. ACS Nano, 2022, 16, 8128
[45] Liu Z, Chen G, Liang B, et al. Fabrication of high-quality ZnTe nanowires toward high-performance rigid/flexible visible-light photodetectors. Opt Express, 2013, 21, 7799
[46] Yao Y, Huang W, Chen J H, et al. Flexible complementary circuits operating at sub-0.5V via hybrid organic-inorganic electrolyte-gated transistors. Proc Natl Acad Sci USA, 2021, 118, 44

Zixu Sa got his BS from ShanDong Normal University in 2021. Now he is a MS student at Shandong University under the supervision of Prof. Zaixing Yang. His research focuses on low-dimension semiconductor device.

Zaixing Yang got his PhD degree in 2012 at Nanjing University. Then he joined City University of Hong Kong as a postdoc. In October 2016, he joined Shandong University as a full professor. His research interest includes low-dimensional optoelectronic materials and devices.